Available online at www.sciencedirect.com
SCIENCE DIRECT®
Coordination Chemistry Reviews 248 (2004) 1215–1224
COORDINATION CHEMISTRY REVIEWS
www.elsevier.com/locate/ccr

Review

Interfacial processes in the dye-sensitized solar cell

Brian A. Gregg*

National Renewable Energy Laboratory, 1617 Cole Boulevard, Golden, CO 80401, USA

Received 25 August 2003; accepted 9 February 2004
Available online 12 April 2004

Contents

Abstract

Interfacial energetics and kinetics are far more important in dye-sensitized solar cells than in conventional solar cells. The huge interfacial area of the nanoporous semiconductor device, with electrolyte permeation throughout the bulk, results in a number of unusual physical characteristics. For example: dark currents can no longer be quantitatively compared to photocurrents; both equilibrium and photoinduced electric fields are rapidly screened throughout the bulk of the cell; the energetics for the crucial processes of electron injection, charge separation and charge recombination are not fixed but depend on a number of dynamic variables; and the open circuit photovoltage is controlled by the photoinduced interfacial chemical potential gradient instead of the built-in equilibrium potential difference. Surface states induced by UV illumination can enhance the photoconversion process in contrast to their detrimental role in conventional cells. Finally, recombination rates can be substantially decreased by modifying the semiconductor/electrolyte interface, rather than by optimizing bulk properties. These effects are described and explained.

Keywords: Dye-sensitized solar cell; Mechanism; Interface; Chemical potential; Recombination

1. Introduction

Dye-sensitized solar cells [1–4], DSSCs or dye cells, are the most promising alternative to conventional solar cells conceived in recent years. They also function by a much different mechanism than conventional solar cells, a mechanism that emphasizes interfacial processes rather than the bulk processes that mostly control silicon p–n junctions and other conventional cells. Conventional photovoltaic (PV) cells are minority carrier devices with planar interfaces/junctions in which both electrons and holes coexist in the same chemical phase: their efficiency is therefore determined by the ability of photogenerated minority carriers (say, electrons in a p-type material) to escape from that side of the device before recombining with the majority carriers [5]. Interfaces are also important in these devices, but the essential processes of photogeneration, separation and recombination of charge carriers all occur primarily in the bulk material. Therefore, bulk properties such as crystallinity and chemical purity often control the efficiency of conventional solar cells, and optimizing these properties can be expensive.

Dye cells, on the other hand, are a special class of majority carrier devices in which the density of minority carriers

* Tel.: +1-303-384-6635; fax: +1-303-384-6632.
E-mail address: brian_gregg@nrel.gov (B.A. Gregg).

0010-8545/$ – see front matter © 2004 Elsevier B.V. All rights reserved.
doi:10.1016/j.ccr.2004.02.009

is insignificant: electrons are found almost exclusively in one phase and holes in another. Charge carriers are generated at the heterointerface between the electron-conducting and hole-conducting phases via light absorption by the sensitizing dye and subsequent photoinjection of an electron into the semiconductor and hole injection into the solution. This interfacial mode of carrier generation is fundamentally different from the bulk generation occurring in conventional cells and is responsible for many of the unusual features of dye cells (and most other organic-based solar cells) [5,6]. Photogeneration, separation and recombination occur almost exclusively at the heterointerface in dye cells, and thus the properties of these interfaces are of paramount importance, while bulk properties are less critical. This allows the use of less pure and therefore less expensive materials. In most other "excitonic" solar cells [6], photogenerated excitons (mobile excited states) must diffuse to the interface before dissociating. In DSSCs, however, the excited states are created right at the interface. The lack of exciton diffusion in DSSCs, and the absence of significant electric fields, make DSSCs the conceptually simplest of the excitonic solar cells and the cell type best able to provide unambiguous answers to some fundamental questions.

Photoelectrochemical (PEC) cells [7–9] represent a class intermediate between conventional solid state p–n junction cells and DSSCs. They usually involve a single crystal semiconductor electrode immersed in an electrolyte and electrically connected thereby to a counter electrode; they may be dye-sensitized, or the semiconductor itself may absorb the light. In the latter case, PEC cells are quite similar to conventional PV cells in the sense that charge generation, separation and much of recombination occur in the bulk semiconductor which has a Schottky junction at the semiconductor-solution interface to separate charges. Still, interfacial properties are crucial to such devices because the surface states are often recombination centers. Dye-sensitized PEC cells [10–13] were the first examples of DSSCs, although they were quite inefficient because they relied on only a monolayer of dye on a planar semiconductor surface to absorb light. In this case, charge generation and separation are similar to what occurs in the nanocrystalline DSSCs, but charge separation is still driven by the internal electric field (band bending) [14,15] which is not available to the Grätzel-type DSSC.

For the most part we distinguish only between conventional cells such as silicon p–n junctions and Grätzel-type DSSCs. In a few cases, we make comparisons to PEC cells.

2. Interpenetrating bicontinuous phases

A fundamental feature of the DSSC is that electrical potentials are strongly screened by the electrolyte solution. The nanostructuring of the TiO_2 substrate allows electrolyte ions to move throughout the "bulk" of the device and thus neutralize all electric fields, equilibrium or photoinduced, within ~1 nm throughout the bulk of the device and within at most a particle diameter, ~15 nm, at the substrate surface. This apparently simple feature has a multitude of consequences and makes the DSSC fundamentally different from conventional semiconductor solar cells which rely entirely on the internal ("built-in") electric field to function [5].

We discuss ionic screening in the next section; but there is also another type of electrical screening. This results from the interpenetrating bicontinuous phases (semiconductor and redox solution) that is characterisic of a DSSC (and of bulk heterojunction devices [16,17]). The two phases have different conductivities and polarizabilities, and those of the semiconductor are highly dependent on light intensity, wavelength and applied potential. Therefore, the average path that the current follows through the device will also depend on these variables. The current will take the distributed path of least resistance (or least impedance for oscillatory potentials). It is possible to use a simple distributed resistor model (Fig. 1) to show that the steady state potentials applied to the electrodes of a DSSC are often strongly screened near the electrodes because the electrolyte is much more conductive than the TiO_2 in the dark [15,18,19]. Upon illumination, however, both the electron concentration *and* the electron diffusion coefficient in the TiO_2 increase by three to four orders of magnitude over a cell at equilibrium [20], meaning that the conductivity of the TiO_2 should increase by six to eight orders of magnitude upon illumination. In this case the applied potential extends much deeper into the device. The spatial extent of the applied potential also depends strongly on the rate constant for interfacial electron transfer across the TiO_2/solution interface [15]. In conven-

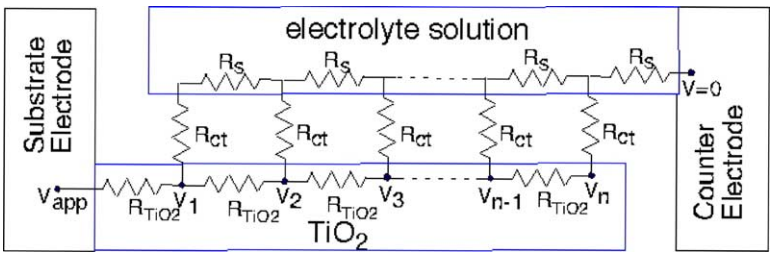

Fig. 1. This distributed resistor network models approximately how the applied potential is distributed across a DSSC under steady state conditions. This is purely an electrical model that does not take mobile electrolyte into account, therefore, potentials at the nodes are electrical potentials, whereas in a true DSSC, all internal potentials are electrochemical in nature.

tional (planar junction) solar cells there is only one possible current pathway, so a simple one-dimensional spatial model is appropriate. But DSSCs are far more complex and require careful consideration of their convoluted geometry.

The complexities resulting from the interpenetration of two continuous (semi)conducting phases also eliminate the possibility of quantitatively comparing the dark currents to the photocurrents, which is a primary analytical tool used with conventional solar cells. The dark current will follow a different average pathway through the cell than the photocurrent, as described above. Furthermore, the dark current and photocurrent are governed by different mechanisms: the dark current is controlled by carrier injection from the electrodes, while the photocurrent is controlled by photoinjection from the dye and recombination processes at the TiO_2/solution interface. These two processes are distinct and occur at different interfaces. Therefore, it is not possible to gain a quantitative understanding of the DSSC photovoltaic behavior by studying its characteristics in the dark. Nevertheless, a qualitative comparison is still possible: the lower the dark current, the higher the possible photovoltage [21].

3. Electrical potentials screened by ion motion

The distributed resistor model neglects (partially) the effect of mobile electrolyte ions, and much of our following discussion of the electrolyte's influence neglects the distributed resistance for simplicity. In a real dye cell, of course, both effects operate simultaneously.

The energy stored in an electric field is minimized by minimizing the spatial extent of the field. Adding electrolyte to a solution contained between charged electrodes will thus decrease the spatial extent of the field as ions flow to constrain the electric field to the smallest volume consistent with the corresponding decrease in entropy of the ions. Therefore, the potential applied to a DSSC electrode will usually drop over just a fraction of the TiO_2 film. It requires energy to expand the electric field into a greater volume. This can be accomplished, for example, by adding electrons to the TiO_2 film, making it more conductive and increasing the amount of stored charge (capacitance) in the electrochemical double layer. We investigated such effects of electrolyte motion experimentally in order to both qualitatively and quantitatively understand the changes in semiconductor physics caused by the migration of ions throughout the "bulk" of a semiconductor device [15,22].

Impedance spectra of DSSCs [22] in the dark with an inert electrolyte showed that the TiO_2 films were not electroactive in the potential range from $+1.0$ V to about the TiO_2 conduction band edge potential at -0.5 V versus SCE. The capacitance in this range was dominated by the planar SnO_2 electrode/electrolyte interface. At potentials more negative than -0.5 V, the TiO_2 becomes progressively more conductive and the electroactive surface area of the film, as measured by its capacitance, expands to eventually include the entire film thickness. These experiments show that even when the interfacial charge transfer rate is minimized by use of inert electrolyte, macroscopic ion motion through the nanoporous film causes the applied potential to drop near the substrate electrode in non-illuminated DSSCs [15].

The *nanoscopic* motion of ions in the pores of a DSSC also plays an important role in the charge separation process. When the photoinjection process produces an electron–hole pair separated across the TiO_2/solution interface, the electrostatic attraction between the opposite charges opposes the separation and promotes recombination. In conventional solar cells this is overcome by the high electric field resulting from the p–n junction. The interior of the dye cell, however, contains no significant electric fields, except across the electrochemical double layers, and these are not adequate to screen an injected electron from the "hole" on the oxidized dye [23,24]. Therefore, a transient attractive electric field is created upon photoinjection that must be rapidly neutralized in order to prevent charge recombination.

In the "standard" DSSC, mobile electrolyte ions can rapidly rearrange around the photogenerated charge pairs, neutralizing the Coulomb attraction between them [14,22] (with some help from the solvent dielectric properties). This is one of the critical functions of the mobile electrolyte in a dye cell. Partly for this reason, it is not trivial to make an efficient solid state version of the dye cell. The required screening of the Coulomb attraction between photogenerated charge carrier pairs is only effective when electrolyte ions can practically surround the charge carrier pair. This was not possible in early versions of solid state dye cells because they lacked mobile electrolyte [17]. The necessary electrostatic screening also cannot occur with dye-sensitized planar semiconductor electrodes [10,11,13], which therefore require a built-in electric field (band bending) to produce a measurable photoconversion effect. However, in the nanostructured geometry of a DSSC, where ions surround the semiconductor particles, no interfacial electric field is required (or even possible in such small colloids) to affect charge separation.

4. Interfacial energies are unpinned

DSSCs are unique in that the photoactive species (the sensitizing dye) resides in the electrochemical double layer between the TiO_2 and the electrolyte solution [14,22,25]. Therefore, the thermodynamic driving forces for all of the crucial interfacial reactions—photoinjection, transfer of the "hole" to solution and carrier recombination—are dependent on the semiconductor band edge potential, the solution redox potential, and on the spatial extent of the potential (double layer) in the interfacial region. The double layer, in turn, is influenced by the species adsorbed to the TiO_2 (including the dye), and by the concentration, chemical nature and physical size of the electrolyte ions. Changing the composition of the electrolyte can thus substantially affect

the photoconversion process by altering the energetics of the interfacial charge transfer reactions. The sensitivity of the interfacial energetics to these many variables adds further complexity to the DSSCs; yet at the same time, it also provides possibilities for optimizing their efficiency.

We proved the somewhat surprising result that the redox potential of the sensitizing dyes become pH-dependent when adsorbed to oxide surfaces, although they are independent of pH when dissolved in solution [14,25]. The conduction band potential of an oxide semiconductor is well-known to move 59 mV/pH unit at room temperature [8,26,27]. This occurs because of the charge induced on the semiconductor surface in equilibrium with the ions in solution: the surface acquires a positive charge in acidic solution and a negative charge in basic solution. We observed that the magnitude of the induced pH-sensitivity of the sensitizing dyes adsorbed onto TiO_2 varied between 54 and 20 mV/pH. The essential parameter appeared to be the location of the redox-active center of the dye in the field of the electrical double layer at the semiconductor/solution interface. If the dye were completely inside the field, as is the TiO_2, its potential would shift the same 59 mV/pH unit as any oxide surface [25,26]. But a species adsorbed on the surface of the TiO_2 cannot be completely inside the double layer field and thus can experience only some fraction of it, depending on the location of the redox center between the surface and the loci of centers of the counterions.

Our explanation of this affect in aqueous solution depended only on geometrical and electrostatic factors, not chemical considerations [25]. Thus, we predicted that similar effects should be observed under appropriate conditions in non-aqueous solvents. By employing two electrolytes with vastly different cation sizes, $LiClO_4$ and $TBAClO_4$ (TBA: tetrabutylammonium) [14], we were able to vary the width of the space charge layer, with the dye located more (TBA^+) or less (Li^+) inside it (Fig. 2). Overall, the results were consistent with the mechanism proposed for the induced pH-sensitivity and showed clearly that interfacial electrostatics, and band edge motion of the semiconductor, play crucial roles in determining the relative potentials (driving forces) in DSSCs. These results are not dependent on the nanostructuring of the interface.

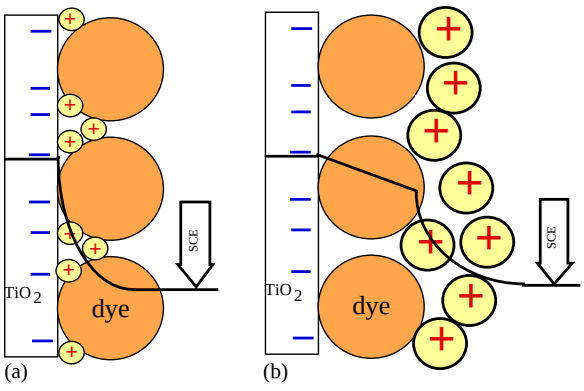

Fig. 2. TiO_2/dye/solution interface shown under negative applied or photogenerated bias. The solid line shows the electrical potential drop between the TiO_2 and the solution. (a) In the presence of small cations, the dye oxidation potential is only slightly affected by changes in the TiO_2 potential. (b) In the presence of large cations, the dye potential follows, but always lags somewhat, changes in the TiO_2 potential.

Our experiments, and the model of Fig. 2, show that the redox potential of the sensitizing dye is not fixed relative to either the semiconductor or the solution, and that the semiconductor band edge is also not fixed. This has important implications for the understanding and optimization of the dye cell. For example, during the course of a potential scan from short circuit to open circuit, the redox potential of the dye in an illuminated cell is expected to move relative to either the TiO_2 or the solution, or both. In the presence of small cations, Fig. 2a, the driving force for charge injection will decrease as the cell approaches its open circuit photovoltage because the semiconductor band edge is charging negative while the dye potential remains relatively constant. But in the presence of large cations, Fig. 2b, the dye will tend to follow the semiconductor potential; thus the driving force for the oxidation of I^- by the oxidized dye will decrease with increasing photopotential. Therefore, the photovoltage-limiting kinetic step may be altered merely by changing the size of the electrolyte cation [14]. The implications of the variable interfacial potentials and driving forces have not yet been rigorously explored; but it is clear that they play an important and subtle role in the functioning of a DSSC. Moreover, the exploitation of these effects may lead to higher efficiency cells.

5. Photoinduced chemical potentials drive the PV effect

Conventional solar cells, almost by definition, all function according to the same photoconversion mechanism epitomized by the photoconversion process in silicon p–n junction PV cells [28,29]. This mechanism is so well known that the assumptions underlying it are sometimes forgotten and it is thought to be the only possible mechanism for photoconversion. But dye cells are different. Here, in the spirit of non-equilibriium thermodynamics, the forces that drive a flux of electrons through a solar cell are described.

Gibbs defined the electrochemical potential energy, E, as the sum of the electrical and chemical potential energies, $E = U + \mu$ [30]. The spatial gradient of a potential energy is a force; and ∇E is ultimately the force that drives the particle fluxes through solar cells and other devices. In solar cells, the gradients of the quasi Fermi levels for each relevant particle, say for electrons, ∇E_{Fn}, and for holes, ∇E_{Fp}, are the forces that drive the particle fluxes. The general kinetic expresssion for the one dimensional current density of electrons, $J_n(x)$, through any device is:

$$J_n(x) = n(x)\mu_n \nabla U(x) + kT\mu_n \nabla n(x) \quad (1)$$

where $n(x)$ is the concentration of electrons, μ_n the electron mobility (not to be confused with the chemical potential, μ) and k and T are Boltzmann's constant and the absolute temperature, respectively. (We assume an effective one-dimensional geometry for simplicity.) There is an exactly analogous equation to describe the flux of holes so, for simplicity, we treat only electrons. Eq. (1) is valid both at equilibrium and away from it, both in the dark and in the light.

The quasi Fermi level (i.e., the non-equilibrium Fermi level) for electrons in a semiconductor is defined as:

$$E_{Fn}(x) = E_{cb}(x) + kT \ln \left\{ \frac{n(x)}{N_c} \right\} \quad (2)$$

where $E_{cb}(x)$ is the electrical potential energy of the conduction band edge, $E_{cb}(x) = U(x) + \text{constant}$; and N_c the density of electronic states at the bottom of the conduction band. Taking the gradient of Eq. (2) and substituting it into Eq. (1) leads to the simplest expression for the electron current through a device:

$$J_n(x) = n(x)\mu_n \nabla E_{Fn}(x) \quad (3)$$

This derivation is based only on kinetic equations and definitions and therefore is valid under non-equilibrium conditions. It is useful to break ∇E_{Fn} into its quasi-thermodynamic constituents, ∇U and $\nabla \mu$, to reveal the fundamental differences between the photoconversion mechanisms of DSSCs and conventional solar cells [5,15]. Eq. (1) can be separated into two independent electron fluxes, each driven by one of the two generalized forces, ∇U and $\nabla \mu$:

$$J_n(x) = n(x)\mu_n(\nabla U(x) + \nabla \mu(x)) \quad (4)$$

where $\nabla \mu(x) = kT/n(x)\, \nabla n(x)$ [5,15]. The first and second terms in parentheses are often referred to as the drift and diffusion components, respectively, of the electron current. One can see immediately from Eq. (4) that $\nabla U(x)$ and $\nabla \mu(x)$ are *independent* forces in the photoconversion process and, therefore, that *it is possible to drive a solar cell with either one, or both, of these forces*. In fact, the different types of solar cells can be classified according to the relative importance of these two forces in the photoconversion process [6].

The gradient of the chemical potential usually plays an insignificant role in conventional PV cells because both electrons and holes are photogenerated together in the same semiconductor phase, and because the carrier mobility is high enough for the carrier distribution to "equilibrate" during the carrier lifetime [5]. Therefore, the rule for conventional solar cells is that the "built-in" potential Φ_{bi} ($=\int \nabla U \, dx$ at equilibrium) sets the absolute upper limit to the open circuit photovoltage, V_{oc}. This occurs because Φ_{bi} is *required* for charge separation. In DSSCs however, the charge carrier pairs are already separated across an interface upon photogeneration, generating a large $\nabla \mu$ (Fig. 3), and ∇U is almost completely screened by the electrolyte. Therefore, these cells are controlled primarily by the photoinduced $\nabla \mu$, and V_{oc} is not limited to Φ_{bi} [5,6,15,31].

This conclusion is now mostly accepted [24,32]. Nevertheless, some still contest it and believe that DSSCs can be treated in the same way as conventional p–n heterojunctions [33–36]. In our view, however, the "contestors" have yet to produce any substantial experimental or theoretical support for their position. We have shown experimentally that the photovoltage of DSSCs is practically independent of the "built-in" potential (Fig. 4). This is in direct contradiction to the "p–n junction model". We have also shown theoretically that there are several reasons to expect that the junction model cannot describe DSSCs [5,6].

6. UV-produced surface states can improve interfacial energetics and transport

Surface states in conventional semiconductor solar cells are almost always deleterious to their performance. But the nanostructured interface of a DSSC makes even this mainstay of conventional understanding incorrect in some cases [37]. We showed that UV illumination of DSSCs results in a remarkable increase in the perfor-

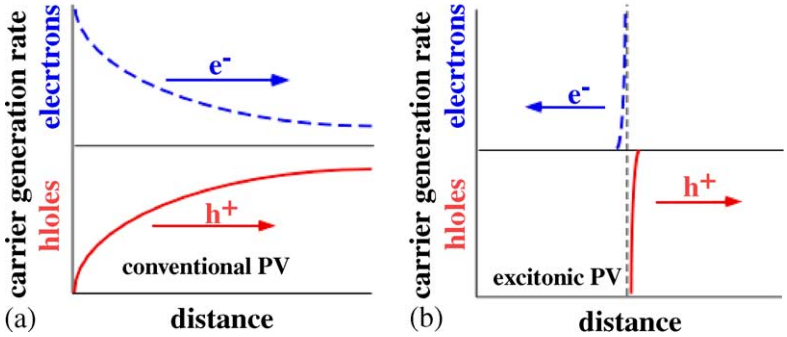

Fig. 3. An illustration of the fundamental difference in charge carrier generation mechanisms in conventional (a) and in excitonic (b) solar cells. In conventional solar cells (a), electrons and holes are photogenerated together wherever light is absorbed. Therefore, the photoinduced chemical potential energy gradient, $\nabla \mu$ (represented by arrows), drives both carrier types in the same direction (although it has a greater influence on minority carriers). In the excitonic cell (b), electrons are photogenerated in one phase while holes are generated in the other via interfacial exciton dissociation (the phase boundary is denoted by the vertical dashed line).

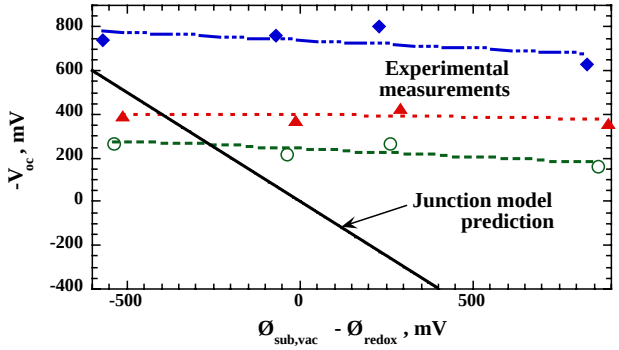

Fig. 4. The open circuit photovoltage at 75 mW/cm^2 incident white light intensity plotted vs. the difference between the work function of the substrate in vacuum, $\Phi_{sub,vac}$, and the solution redox potential, Φ_{redox}. The four types of substrates are, from left to right, ITO, SnO_2, Au and Pt; the filled diamonds are for 0.5 M LiI solution, the open circles are for 0.05 M ferrocene in 0.1 M $LiClO_4$ solution and the filled triangles are for 0.05 M hydroquinone in 0.1 M $LiClO_4$ solution. The theoretical line shows the behavior predicted by the junction model. (Data from ref. [31].)

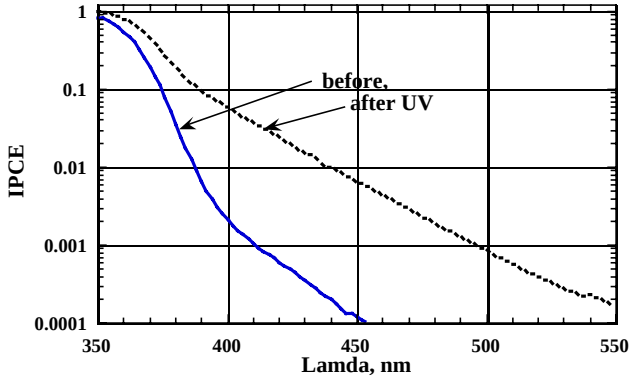

Fig. 6. Photocurrent action spectra of bare TiO_2 film before and after 15 min of UV illumination showing the large increase in photoactive, sub-bandgap states induced by UV. This occurs in TBA^+-containing solution but not in Li^+-containing solution. (Data from ref. [37].)

mance for cells (Fig. 5) sensitized with some less-than-optimal dyes such as bis(2,2′-bipyridine) (4,4′-dicarboxylic acid-2,2′-bipyridine)ruthenium(II) [37,38]. The more common sensitizing dye is "N3", bis(4,4′-dicarboxy-2,2′-bipyridine)ruthenium(II) di-isothiocyanate. The first dye (that we refer to as the "tris dye") has a more positive redox potential than N3 and a relatively poor photoconversion efficiency before UV illumination in the usual cell. UV illumination can even more drastically increase the efficiency of some perylene-based sensitizing dyes [39,40]. The efficiency of cells made with some of the perylene dyes increase (quasi-permanently) by up to 45-fold upon illumination with UV light. Given the huge changes in behavior of these DSSCs upon UV illumination, we carried out a detailed study of this effect [37].

We quickly learned that this effect occurred only in the presence of non-adsorbing cations such as tetrabutyl ammonium, TBA^+, and that it was inhibited by the usual cation, Li^+. The obvious difference between these cations is that Li^+ specifically adsorbs to the TiO_2, and thus chemically modifies its surface, while TBA^+ does not chemically interact with the TiO_2 surface. We showed that larger cations that adsorb to some extent, such as Na^+ and K^+ also inhibit the UV effect to the extent that they adsorb. These and other results suggested that the effect resulted from a UV-induced change in the TiO_2/electrolyte interface and was not related to the sensitizing dye [37]. Measurements of the IPCE (incident photon to current efficiency) on nanocrystalline TiO_2 cells without sensitizing dye showed a remarkable increase in sub-bandgap current upon UV illumination (Fig. 6) in the presence of TBA^+ electrolyte but not in the presence of Li^+ electrolyte. The half-life of the changes caused by UV illumination was several months in a sealed cell.

The surprising increase in photocurrent under visible light irradiation ($\lambda > 400$ nm) after UV illumination of the unsensitized cell in TBA electrolyte (Fig. 6) shows that photoactive sub-bandgap states are created upon UV illumination. In both TBA and Li cells, IPCE measurements before UV illumination showed the expected spectrum of a semiconductor with a ~3.2 eV bandgap, demonstrating that neither

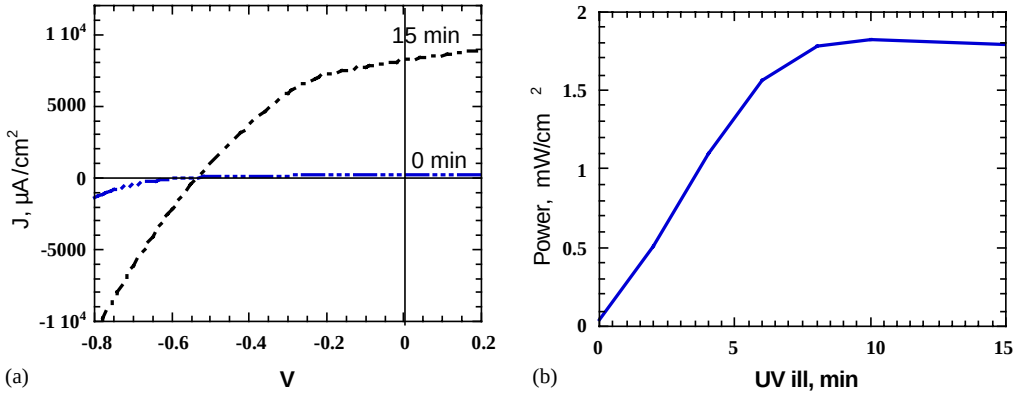

Fig. 5. (a) Photocurrent-voltage characteristics of a tris-dye-sensitized cell before and after 15 min of UV illumination. (b) The change in power produced in the cell with UV illumination time. (Data from ref. [37].)

Li^+ nor TBA^+ by itself perturbs the photoactive electronic structure of the TiO_2 surface. However, after UV illumination, the bare TiO_2 films produce a ~10–100-fold increase in photocurrent below E_{cb} in the TBA-cells (Fig. 6), while a slight *decrease* in photocurrent is observed in the Li cells (not shown).

The change in TBA-cells upon UV illumination (Fig. 6) is a highly unusual result that reveals visually the presence of photoactive surface states [37]. Most commonly, the presence of semiconductor surface states is not directly seen and only can be inferred via indirect measurements and comparison to theory. However, here we observe a clear spectroscopic signature of a large density of photoactive surface states that can be produced by UV illumination, and eliminated again by exposure to ambient air. This high density of sub-bandgap states suggests comparisons to the electronic structure of amorphous silicon. Once the density of intragap (or surface) states becomes large enough to accomodate carrier transport, conduction can occur primarily through these sub-bandgap states: therefore, the notion of a distinct bandedge may no longer truly be relevant. In the UV-illuminated nanoporous TiO_2 films, *the mobility edge may be described as the percolation threshold of surface states*, that is, as that energy level at which the surface state density becomes high enough to support a current flux. In planar (conventional) semiconductor electrodes, intragap surface states are almost always harmful. Since there is no direct physical connection between the surface and the substrate electrical contact, surface states are always trap states, regardless of their concentration. Ionization of the surface states (say, their filling by electrons) results in charging of the surface and bandedge motion (Fermi level pinning). It is usually concluded that a higher density of surface states therefore leads to a greater degree of bandedge motion under illumination. However, this conclusion is not fundamental; it applies only to *planar* semiconductor electrodes. Bandedge motion is caused by the steady state *charge* density at the surface, not by the surface state density alone.

In nanostructured semiconductor electrodes, the surface extends throughout the "bulk". Therefore, surface states can be in direct electrical contact with the substrate. Before UV illumination, most surface states in the nanoporous TiO_2 may be isolated traps which, when charged with electrons, move the bandedge negative. However, further increasing the density of surface states in DSSCs may lead to electrical communication between the surface states and thereby ultimately to an *improved* conducting pathway to the substrate—a "mobility edge" as mentioned above. Therefore, increasing the surface state density by UV illumination can, in principle, lead to *less* bandedge motion in DSSCs because it results in improved carrier transport and *decreased charge density* at the surface. As more surface states are created and they begin to coalesce into a mobility edge, the effective bandedge moves positive from E_{cb} to the mobility edge, and carrier transport may become more efficient, thus decreasing the total charge on the surface. This mechanism is still speculative, but it is consistent with all of our results regarding the UV effect. Regardless of mechanism, all the results show that UV illumination alters the interfacial energetics and/or kinetics. A practical advantage is thus the ability to adjust the essential photoconversion parameters, J_{sc}, V_{oc}, ff, etc., to maximize the conversion efficiencies.

7. Interfacial recombination

The recombination of photogenerated electrons and holes is the bane of all solar cells and a major reason for their less than ideal efficiencies. DSSCs, in which the electrons and holes exist in separate chemical phases, are subject almost exclusively to interfacial recombination. In principle, interfacial recombination processes can be inhibited by modifying the interface. The use of *t*-butylpyridine in the DSSC electrolyte solution to increase its photovoltage is one example [2,41]. We explored general methods for passivating interfacial recombination sites in DSSCs that might allow the use of a variety of redox couples, and thereby facilitate making a viable solid state DSSC.

Only one redox couple, I^-/I_2, allows conventional dye-sensitized solar cells to function efficiently because of the uniquely slow kinetics for I_2 reduction on SnO_2 and TiO_2 surfaces. The reduction is so slow at both TiO_2 [42] and SnO_2 surfaces [21] that almost every electron photoinjected into the TiO_2 at short circuit survives the transit through the nanoporous film and the SnO_2 substrate and appears in the external circuit. Only recently, have other couples with ultra-slow kinetics been discovered. Cells made with these couples are not yet as efficient as those made with I^-/I_2 [43–45].

We sought a general method to inhibit recombination in DSSCs. To gauge our success, we required a redox couple with a heterogeneous electron transfer rate so fast that the interfacial recombination process would become the photocurrent-limiting reaction. Therefore, we employed the kinetically very fast ferrocene/ferrocenium couple ($FeCp_2^{+/0}$, self-exchange rate, $k_{ex} \approx 10^7\,M^{-1}\,s^{-1}$) [46] compared to the I^-/I_2 couple ($k_{ex} \approx 5 \times 10^2\,M^{-1}\,s^{-1}$) [47]. It has a redox potential only slightly more positive than the iodine couple (0.31 V versus SCE compared to ~0.15 V). The recombination reactions in DSSCs can be qualitatively understood by measuring the dark currents of DSSCs in both I^-/I_2 and $FeCp_2^{+/0}$ containing electrolyte solutions (Fig. 7). A quantitative understanding is not possible yet, as discussed above. In I^-/I_2 solutions, the dark current increases with an overpotential of ~0.4 V for I_2 reduction. However, in $FeCp_2^{+/0}$ solution, the overpotential disappears and the dark current is substantial even at ±10 mV [21].

The dark *J–V* curves with the I^-/I_2 couple appear to be "diode-like" (Fig. 7). But this is actually caused by a kinetic overpotential rather than by the electrical potential, Φ_{bi}, of a semiconductor junction. This is easily seen by

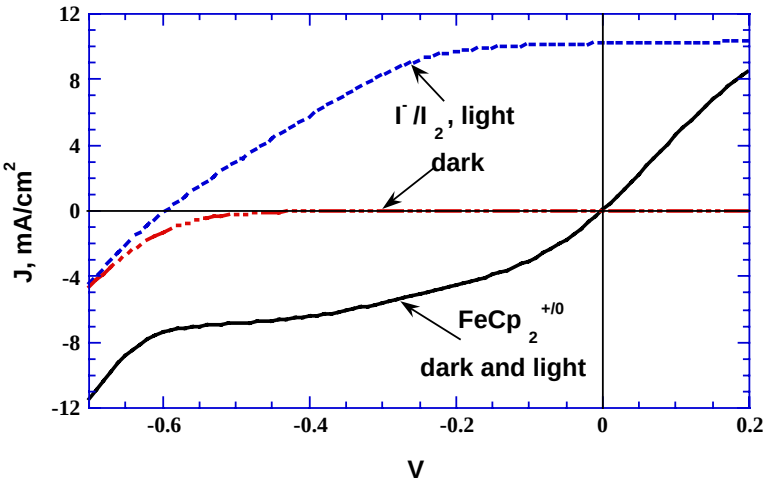

Fig. 7. Current-voltage curves of a DSSC in the light and dark employing the kinetically slow redox couple, I^-/I_2, and the kinetically fast couple $FeCp_2^{+/0}$. (Data from ref. [21].)

comparing the curves for the two redox couples. The apparent diode-like character disappears with the kinetically fast couple, $FeCp_2^{+/0}$, even though its more positive redox potential would be expected to *increase* Φ_{bi} of the putative junction and thus enhance its diode-like behavior.

When we derivatize the solvent-exposed oxide interfaces with an electrical insulator (described below), this cannot create an electrical junction. Yet it does impart "diode-like" character to the dark and light currents measured with $FeCp_2^{+/0}$. That is, derivitization *creates an electrochemical overpotential* for the recombination reactions; just as there is naturally an electrochemical overpotential for the reduction of I_2/I_3^-. In general, slowing the rate of the recombination reaction(s) relative to the photodriven forward reactions, by whatever mechanism, establishes the necessary conditions for a successful photoconversion process.

The photocurrent–voltage curve of a cell made with the I^-/I_2 redox couple (Fig. 7) shows behavior typical of the standard DSSC. A substantial photovoltaic effect is observed as expected from the fact that the dark current is negligible positive of about −0.5 V. On the other hand, a cell made with the $FeCp_2^{+/0}$ redox couple shows no measurable photoeffect: its current under illumination (Fig. 7) is essentially identical to its dark current. The photovoltaic effect is negligible because practically all photogenerated charge carriers recombine before they can be collected in the external circuit.

There are two major recombination reactions of importance to a DSSC: the recombination of the photoinjected electron with the oxidized redox species at the SnO_2/solution interface and at the TiO_2/solution interface. The first reaction is easily inhibited by electropolymerizing an insulating film on the solvent-exposed parts of the SnO_2 after the nanocrystalline TiO_2 film has been deposited but before the dye is adsorbed [21]. We electrodeposited a blocking layer of crosslinked poly(phenyleneoxide-co-2-allylphenyleneoxide) on the TiO2-coated SnO_2 surface by adapting a literature procedure [48]. This has a pronounced effect on the *J–V* characteristics of a DSSC employing $FeCp_2^{+/0}$: the dark current is reduced by two to three orders of magnitude in the potential range positive of the TiO_2 flatband, and the photocurrent increases from 0 to 0.5 mA/cm^2 [21].

The sensitizing dye cannot cover all of the TiO_2 surface. Because of its very high surface area, it is most important to passify recombination on the solvent-exposed parts of the TiO_2. We developed a chemical reaction that covered the exposed oxide surfaces with an ultrathin electrically insulating film. We employed CH_3SiCl_3 in the vapor phase: it forms covalently bound films of poly(methylsiloxane) on the exposed surfaces of both TiO_2 and SnO_2 films [21]. Although the conditions for this reaction have not been optimized, substantial decreases in the rates of the recombination reactions, and increases in photoconversion efficiencies, could be achieved (Fig. 8).

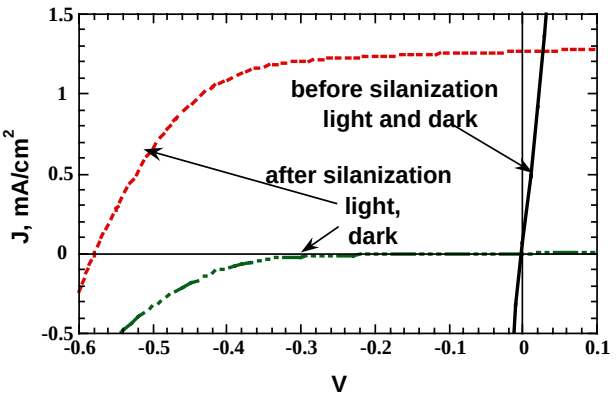

Fig. 8. Dark and photocurrent-voltage curves in $FeCp_2^{+/0}$ solution before and after silanization to passivate the recombination sites on the TiO_2 and SnO_2 surfaces. (Data from ref. [21].)

These results demonstrate two important points: (1) The recombination reactions in DSSCs are fundamentally different than those occurring in conventional solar cells and therefore, very different methods must be employed to minimize them. (2) Physically blocking the sites where the oxide is exposed to solution with an electrical insulator can decrease the recombination rate by more than five orders of magnitude. The major difficulty of this technique is preventing capillary condensation of the reactive silane vapor in the nanopores of the TiO_2. With further improvement, this technique should allow the use of any redox couple in the DSSC, thus promoting the development of solid state versions.

8. Summary and conclusions

The dye cell is a nanoporous, interface-driven solar cell that seems to defy conventional wisdom. It contains no substantial built-in electrical potential, $\Phi_{bi} \approx 0$, yet it produces a substantial photovoltage; carrier transport occurs primarily by diffusion rather than by drift, yet it is highly efficient. Most fundamentally, electrons and holes are photogenerated on opposite sides of the interface, already separated into their individual phases, leading to the overwhelming importance of interfacial processes over bulk proceses. In fundamental ways, dye cells contrast with conventional PV cells. The absence of any macroscopic electric fields in DSSCs, as well as the elimination of the requirement for exciton diffusion to the interface, also makes DSSCs in many respects the simplest excitonic solar cells. They were employed to probe the necessity for a built-in electric field, or junction, in solar cells. The results show unambiguously that a built-in electric field is only one of the two possible driving forces in a solar cell. And the other, the photoinduced interfacial chemical potential gradient, is the major driving force for photoconversion in DSSCs.

The nanoporous nature of the dye-sensitized semiconductor in DSSCs results in a complex spatial distribution of applied or photogenerated potential gradients through the cell. Moreover, the nanoscopic motion of electrolyte ions in response to the Coulomb field between photogenerated electrons and holes plays a crucial role in the charge separation process. The fact that the sensitizing dyes reside partially inside the electrochemical double layer at the TiO_2/solution interface leads to the unusual and complex situation where the driving forces for the most important electron transfer reactions vary with potential, light intensity, pH, and even with the size of electrochemically inert counterions and the shape of the dye.

UV illumination of the cells induces the formation of a large density of optically observable surface states. In contrast to surface states in conventional solar cells, these states can dramatically enhance the photoconversion efficiency of DSSCs by providing an improved conducting pathway to the electrode. Because of the interfacial nature of all important charge transfer processes in DSSCs, novel methods of passivating the recombination sites by interface derivitization are possible and preliminary attempts seem promising.

Acknowledgements

I am grateful to all my colleagues and collaborators, most of whom are listed as co-authors in our cited references and to the US Department of Energy, Office of Science, Division of Basic Energy Sciences, Chemical Sciences Division for supporting this research.

References

[1] B. O'Regan, M. Grätzel, Nature 353 (1991) 737.
[2] K. Kalyanasundaram, M. Grätzel, Coord. Chem. Rev. 77 (1998) 347.
[3] M.K. Nazeeruddin, A. Kay, I. Rodicio, R. Humphry-Baker, E. Müller, P. Liska, N. Vlachopoulos, M. Grätzel, J. Am. Chem. Soc. 115 (1993) 6382.
[4] B. O'Regan, J. Moser, M. Anderson, M. Grätzel, J. Phys. Chem. 94 (1990) 8720.
[5] B.A. Gregg, M.C. Hanna, J. Appl. Phys. 93 (2003) 3605.
[6] B.A. Gregg, J. Phys. Chem. B 107 (2003) 4688.
[7] H. Gerischer, Semiconductor electrochemistry, in: Physical Chemistry. An Advanced Treatise, Academic Press, New York, vol. 9A, 1970.
[8] A.J. Nozik, Ann. Rev. Phys. Chem. 29 (1978) 189.
[9] A.J. Bard, Science 207 (1980) 139.
[10] H. Gerischer, Photochem. Photobiol. 16 (1972) 243.
[11] R. Memming, Photochem. Photobiol. 16 (1972) 325.
[12] B.A. Parkinson, M. T. Spitler, Electrochim. Acta 37 (1992) 943.
[13] M.T. Spitler, J. Electroanal. Chem. 228 (1987) 69.
[14] A. Zaban, S. Ferrere, B.A. Gregg, J. Phys. Chem. B 102 (1998) 452.
[15] B.A. Gregg, The essential interface: studies in dye-sensitized solar cells, in: K.S. Schanze, V. Ramamurthy (Eds.), Semiconductor Photochemistry and Photophysics, vol. 10, Marcel Dekker, New York, 2003, p. 51.
[16] W.U. Huynh, X. Peng, A.P. Alivisatos, Adv. Mater. 11 (1999) 923.
[17] S.E. Shaheen, C.J. Brabec, N.S. Sariciftci, F. Padinger, T. Fromherz, Appl. Phys. Lett. 78 (2001) 841.
[18] J. Bisquert, G. Garcia-Belmonte, F. Fabregat-Santiago, J. Solid State Electrochem. 3 (1999) 337.
[19] J. Bisquert, G. Garcia-Belmonte, F. Fabregat-Santiago, N.S. Ferriols, P. Bogdanoff, E.C. Pereira, J. Phys. Chem. B 104 (2000) 2287.
[20] N. Kopidakis, E.A. Schiff, N.-G. Park, J. van de Lagemaat, A.J. Frank, J. Phys. Chem. B 104 (2000) 3930.
[21] B.A. Gregg, F. Pichot, S. Ferrere, C.L. Fields, J. Phys. Chem. B 105 (2001) 1422.
[22] A. Zaban, A. Meier, B.A. Gregg, J. Phys. Chem. B 101 (1997) 7985.
[23] G. Schlichthörl, S.Y. Huang, J. Sprague, A.J. Frank, J. Phys. Chem. B 101 (1997) 8141.
[24] D. Cahen, G. Hodes, M. Grätzel, J.F. Guillemoles, I. Riess, J. Phys. Chem. B 104 (2000) 2053.
[25] A. Zaban, S. Ferrere, J. Sprague, B.A. Gregg, J. Phys. Chem. B 101 (1997) 55.
[26] H. Gerischer, Electrochem. Acta 34 (1989) 1005.
[27] S. Yan, J.T. Hupp, J. Phys. Chem. 100 (1996) 6867.
[28] A.L. Fahrenbruch, R.H. Bube, Fundamentals of Solar Cells. Photovoltaic Solar Energy Conversion, Academic Press, New York, 1983.
[29] M. Green, Adv. Mater. 13 (2001) 1019.
[30] J.W. Gibbs, The Scientific Papers of J. Willard Gibbs, vol. 1, Dover, New York, 1961.

[31] F. Pichot, B.A. Gregg, J. Phys. Chem. B 104 (2000) 6.
[32] J. Ferber, R. Stangl, J. Luther, Solar Energy Mater. Solar Cells 53 (1998) 29.
[33] T. Dittrich, P. Beer, F. Koch, J. Weidmann, I. Lauermann, Appl. Phys. Lett. 73 (1998) 1901.
[34] K. Schwarzburg, F. Willig, J. Phys. Chem. B 103 (1999) 5743.
[35] K. Schwarzburg, F. Willig, J. Phys. Chem. B 107 (2003) 3552.
[36] G. Kron, T. Egerter, J.H. Werner, U. Rau, J. Phys. Chem. B 107 (2003) 3556.
[37] B.A. Gregg, S.-G. Chen, S. Ferrere, J. Phys. Chem. B 107 (2003) 3019.
[38] S. Ferrere, B.A. Gregg, J. Phys. Chem. B 105 (2001) 7602.
[39] S. Ferrere, A. Zaban, B.A. Gregg, J. Phys. Chem. B 101 (1997) 4490.
[40] S. Ferrere, B.A. Gregg, N. J. Chem. 26 (2002) 1155.
[41] A. Kay, R. Humphry-Baker, M. Grätzel, J. Phys. Chem. 98 (1994) 952.
[42] J.S. Salafsky, W.H. Lubberhuizen, E. van Faassen, R.E.I. Schropp, J. Phys. Chem. B 102 (1998) 766.
[43] H. Nusbaumer, J.-E. Moser, S.M. Zakeeruddin, M.K. Nazeeruddin, M. Grätzel, J. Phys. Chem. B 105 (2001) 10461.
[44] G. Oskam, B.V. Bergeron, G.J. Meyer, P.C. Searson, J. Phys. Chem. B 105 (2001) 6867.
[45] S.A. Sapp, C.M. Elliott, C. Contado, S. Caramori, C.A. Bignozzi, J. Am. Chem. Soc. 124 (2002) 11215.
[46] R.M. Penner, M.J. Heben, T.L. Longin, N.L. Lewis, Science 250 (1990) 1118.
[47] J. Sun, D.M. Stanbury, Inorg. Chem. 37 (1998) 1257.
[48] T.G. Strein, A.G. Ewing, Anal. Chem. 64 (1992) 1368.